sciendo DOI: 10.2478/ace-2019-0019 ARCHIVES OF CIVIL ENGINEERING
Vol. LXV ISSUE 2 2019

EXPERIMENTAL AND NUMERICAL STUDY OF THE UNIAXIAL COMPRESSIVE STRESS-STRAIN RELATIONSHIP OF A ROCK MASS WITH TWO PARALLEL JOINTS

L. X. Xiong[1, 2], H. Y. Yuan[3], Y. Zhang[4], K. F. Zhang[3], J. B. Li[3]

A "rock bridge", defined as the closest distance between two joints in a rock mass, is an important feature affecting the jointed rock mass strength. Artificial jointed rock specimens with two parallel joint fractures were tested under uniaxial compression and numerical simulations were carried out to study the effects of the inclination of the rock bridge, the dip angle of the joint, rock bridge length, and the length of joints on the strength of the jointed rock mass. Research results show: (1) When the length of the joint fracture, the length of the rock bridge, and the inclination of the rock bridge stay unchanged, the uniaxial compressive strength of the specimen gradually increases as the inclination of the joint fracture increases from 0°to 90°. (2) When the length of the joint fracture, the length of the rock bridge, and the inclination of the joint fracture stay unchanged, the uniaxial compressive strength of the specimen shows variations in trends with the inclination of the rock bridge increasing from 30° to 150° (3). In the case when the joint is angled from the vertical loading direction, when the dip angle of the joint fracture, the inclination of the rock bridge, and the length of the rock bridge stay unchanged, the uniaxial compressive strength of the specimen gradually decreases with an increasing length of joint fracture. When the dip angle of the joint fracture, the inclination of the rock bridge, and the length of the joint fracture stay unchanged, the uniaxial compressive strength of the specimen does not show a clear trend with an increase of the length of the rock bridge.

Keywords: Jointed rock mass, parallel joints, peak strength

[1] L.X. Xiong, Associate Prof., PhD., Eng., State Key Laboratory of Geohazard Prevention and Geoenvironment Protection, Chengdu University of Technology, Chengdu 610059, PR China, xionglx1982@126.com

[2] L.X. Xiong, Associate Prof., PhD., Eng., Key Laboratory of Geotechnical and Underground Engineering of Ministry of Education, Tongji University, Shanghai 200092, PR China, xionglx1982@126.com

[3] H.Y. Yuan, Graduate student, College of Environment and Civil Engineering, Chengdu University of Technology, Chengdu, 610059, PR China, 1045919790@qq.com

[4] Y. Zhang, Associate Prof., PhD., Eng., Terracon Consultants. 13050 Eastgate Park Way, Louisville, KY, USA. E-mail: zhyao@umich.edu

[3] K. F. Zhang, Graduate student, College of Environment and Civil Engineering, Chengdu University of Technology, Chengdu, 610059, PR China, 1045919790@qq.com

[3] L. B. Li, Graduate student, College of Environment and Civil Engineering, Chengdu University of Technology, Chengdu, 610059, PR China, 1045919790@qq.com

1. INTRODUCTION

Joint fractures are common within rock masses, and the geometric distribution of the joint fractures significantly impacts the strength, deformation, and failure models of the rock mass. Many researchers have performed model tests and numerical simulations to study the strength and deformation characteristics of rock masses with joint fractures, including cross-joint fractures, 2 joint fractures, 3 joint fractures, and multiple sets of parallel joint fractures.

Among these, the undermentioned researchers conducted experiments and numerical simulations on rock masses containing 2 fractured joints. Huang conducted triaxial compression experiments on sandstone samples with two preexisting closed non-overlapping flaws to investigate their deformation and strength behaviors [1]. Li conducted a numerical study on the coalescence of two preexisting parallel open flaws in rock subjected to uniaxial compressive loading [2]. Zhang carried out an experimental and numerical investigation on a double-flawed rock-like specimen subjected to uniaxial compression under different quasi-static strain rates [3]. Zhang conducted a numerical study on the cracking and coalescence behaviors of a rectangular rock-like specimen containing two parallel (stepped and coplanar) pre-existing open flaws under uniaxial compression [4]. Zhao et al. carried out a series of uniaxial compression tests on a rock-like specimen containing two flaws [5]. Yang et al. conducted uniaxial compression experiments to evaluate the influence of ligament angle on the strength, deformability, and fracture coalescence behaviors of rectangular prismatic specimens of brittle sandstone containing two non-coplanar fissures [6-7]. In these experimental and numerical studies on jointed rock mass specimens with two jointed fractures, the scopes of the inclination of the rock bridge, the dip angle of the joint fracture, the length of the rock bridge, and the length of the joint fracture are relatively small.

In this study, uniaxial compression tests and numerical simulations are performed on artificial jointed rock specimens with two parallel equal-length joint fractures to study the effects of the dip angle of the rock bridge, the dip angle of the fracture, the length of the rock bridge, and the length of the joint fracture on the strength characteristics of jointed rock mass.

2. EXPERIMENT SETUP

2.1. SPECIMEN PREPARATION

The specimens used in this study were 10 cm × 10 cm × 10 cm, and the non-persistent joints were generated by inserting planks of 1 mm thickness into the mold after the model materials were set. The uniaxial compressive loading diagram of the jointed rock mass model with two parallel equal-length joint fractures is shown in Fig. 1.

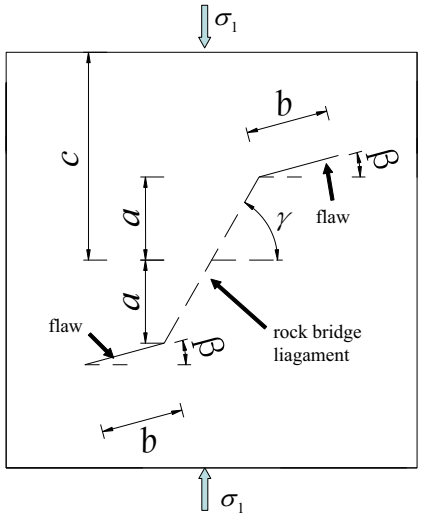

Fig. 1. The uniaxial compressive loading diagram of the joint rock mass specimen with two parallel equal-length fractures.

In this manuscript, the lengths of both joint fractures are designated as b; the angle between each joint fracture and the horizontal plane is defined as β; the distance from the center of the rock bridge to the upper surface of the specimen is 5 cm; the projection length of the rock bridge to the vertical axis is $2a$; the angle between the rock bridge and the horizontal plane is defined as γ. Various values of $2a$, b, β, and γ were selected and studied in this research.

Cement mortar with a water/cement ratio of 0.65 was used to prepare the specimens for this study. No. 425-type cement was used in this study, in accordance with the China Building Materials Academy. ISO standard sand was used and the particle size of the sand ranges from 0.5 mm to 1.0

mm. A wood plank was inserted in the positions marked by the short-line in Fig. 1 after the cement mortar was set. The width of the plank was the same as the length (b) of the joint fracture, the thickness of the plank is 1 mm, and its length is 11 cm. The wood planks reached across the entire specimen, and were left inside the specimen permanently.

2.2. TEST SEQUENCE

After the test specimens were cured for 28 days and placed for 7 days, an unconfined compressive strength (UCS) test was carried out on the specimens at a displacement loading rate of 0.6mm/min using a WAW-600C universal testing machine.

2.3 TEST GROUP

The tests were grouped based on the values of $2a$, b, β, and γ, as shown in Table 1.

Table 1. Test groups with different values of $2a$, b, β, and γ.

Study	$2a$ (cm)	b (cm)	γ (°)	β (°)
1	4	2	30	45, 60, 75, and 90
2	4	2	45	0, 15, 30, 45, 60, 75, and 90
3	4	2	60	0, 15, 30, 45, 60, 75, and 90
4	4	2	75	0, 15, 30, 45, 60, 75, and 90
5	4	2	90	0, 15, 30, 45, 60, 75, and 90
6	4	2	105	0, 15, 30, 45, 60, 75, and 90
7	4	2	120	0, 15, 30, 45, 60, 75, and 90
8	4	2	135	0, 15, 30, 45, 60, 75, and 90
9	4	2	150	0, 15, 30, 45, 60, 75, and 90

3. EVOLUTION OF TEST RESULTS AND ANALYSIS

3.1 THE VARIATION OF THE STRESS-STRAIN CURVES

The uniaxial compression stress-strain curves of the jointed rock specimens for each selected γ with various β values are shown below in Fig. 2.

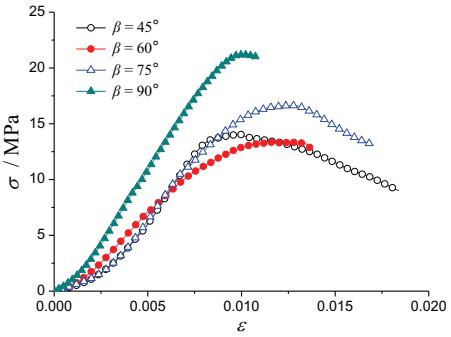

(a) γ =30°

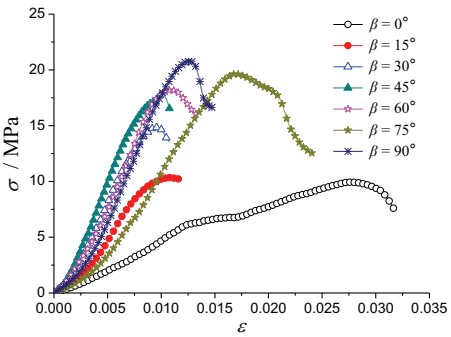

(b) γ = 45°

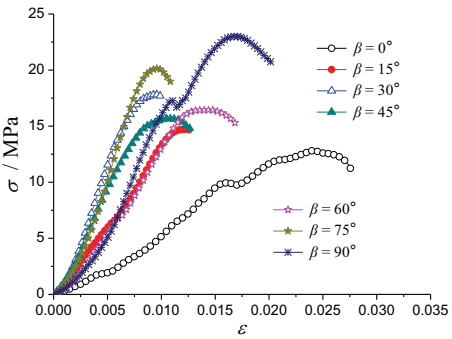

(c) γ = 60°

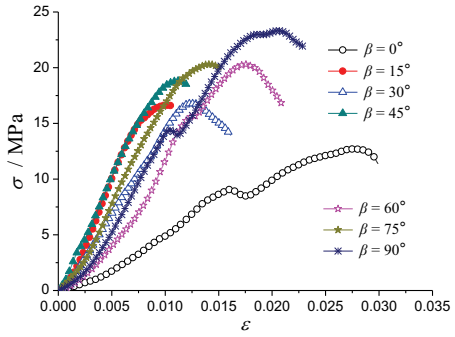

(d) γ = 75°

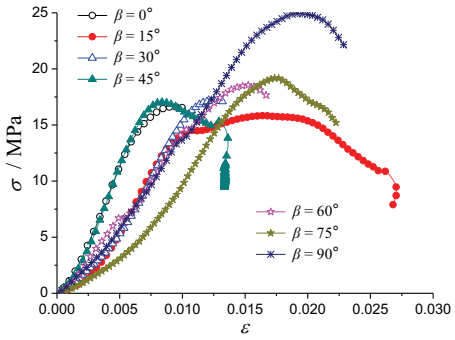

(e) $\gamma = 90^\circ$

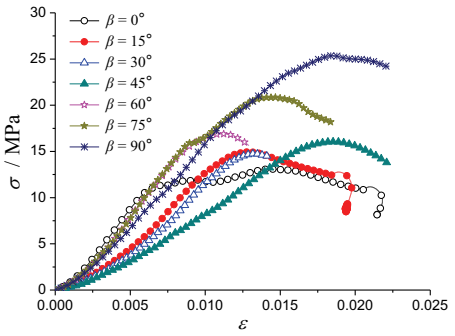

(f) $\gamma = 105^\circ$

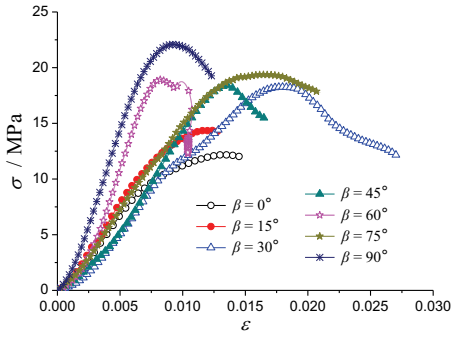

(g) $\gamma = 120^\circ$

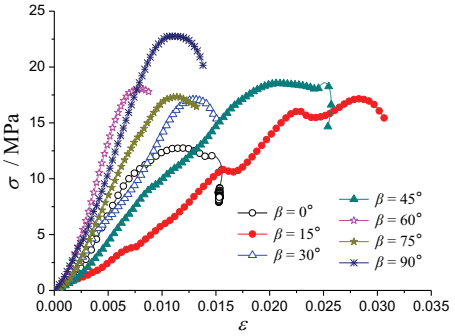

(h) $\gamma = 135^\circ$

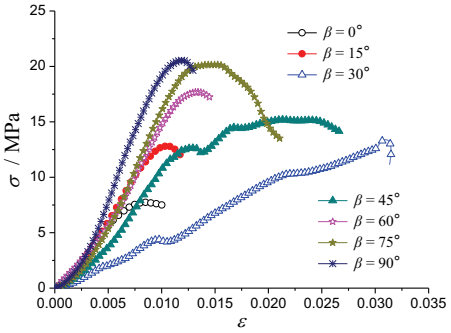

(i) $\gamma = 150^\circ$

Fig. 2. The influence of β on the stress-strain curve of the specimen for each selected γ.

In Fig. 2 it can be seen that when γ is the same and β increases from 0° to 90°, the stress-strain curves are composed mainly of the compaction stage, linear elastic stage, yielding stage, and post-peak softening stage. The peak stress for $\beta = 90°$ is higher than that for $\beta = 0°$.

3.2 THE EVOLUTION OF COMPRESSIVE STRENGTH

The compressive strength takes the peak point of the stress-strain relationship curve. The uniaxial compressive strength of the jointed rock mass specimen for each selected γ with various β values are shown below in Fig. 3.

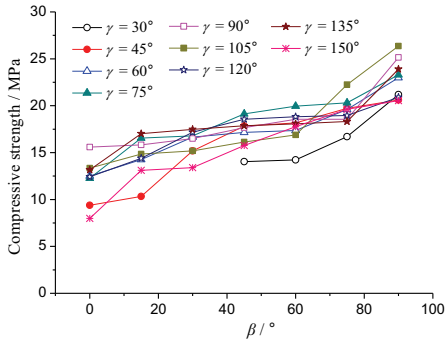

Fig. 3. The influence of β on the uniaxial compressive strength of the specimen for each selected γ.

It can be seen that the uniaxial compressive strength of the specimen gradually increases with β increasing from 0° to 90° when γ remains unchanged.

When angle β remains the same, the influence of angle γ on the uniaxial compressive strength of the jointed rock mass specimen is shown in Fig. 4.

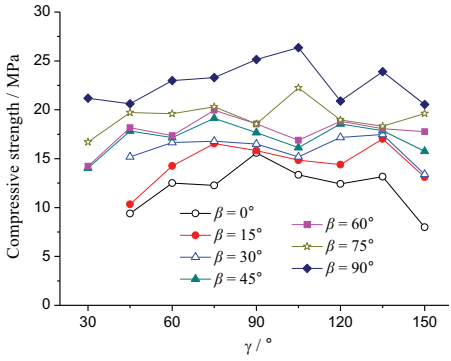

Fig. 4. The influence of β on the uniaxial compressive strength of the specimen when γ is the same.

It can be seen that when β remains unchanged and γ increases from 30° to 150°, the uniaxial compressive strength of the jointed rock specimen increases at first and then decreases.

4. THE COMPARISON BETWEEN THE EXPERIMENTAL AND NUMERICAL RESULTS

4.1. NUMERICAL MODEL

FLAC^{3D} was used for the numerical simulation in this study. The null elements were adopted to simulate the joint planes in the model, thus, there are no mechanical parameters for the joint planes. The 3D model is comprised of an 8-node hexahedral element. When $2a$ = 4 cm, b = 2 cm, and γ = 45°, the simulation models of the jointed rock mass specimens are shown below in Fig. 5.

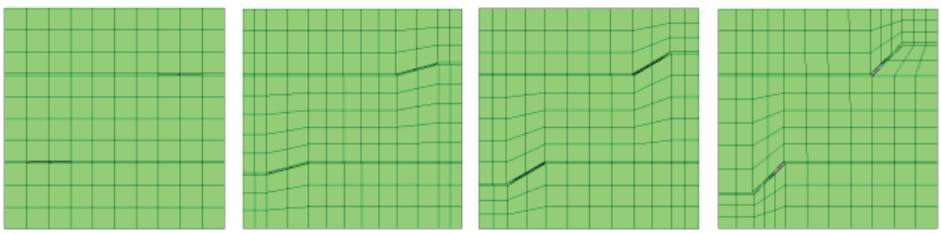

(a) $\beta = 0^\circ$ (b) $\beta = 15^\circ$ (c) $\beta = 30^\circ$ (d) $\beta = 45^\circ$

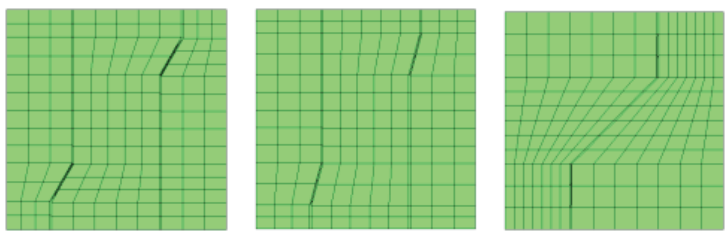

(e) $\beta = 60^\circ$ (f) $\beta = 75^\circ$ (g) $\beta = 90^\circ$

Fig. 5. Numerical models with $2a$ = 4 cm, b = 2 cm, and γ = 45°.

4.2. CONSTITUTIVE MODEL AND MATERIAL PROPERTIES

The Mohr-Coulomb model was used in the numerical analysis. The parameters of the model are obtained mainly according to the test results of $\gamma = 90°$ and $\beta = 90°$. For this case, the calculated values of the compressive strength are consistent with the experimental values. Therefore, material properties for rock-like materials are: bulk modulus K is 8 GPa, shear modulus G is 4.8 GPa, cohesion is 5.0 MPa, the internal friction angle is 47°, and tensile strength is 2.5 MPa.

4.3. COMPARISON OF EXPERIMENTAL AND NUMERICAL RESULTS

For $2a = 4$ cm, and $b = 2$ cm, when γ is kept unchanged and β varies from 0° to 90°, the numerical results of the compressive strength of the specimens are shown below.

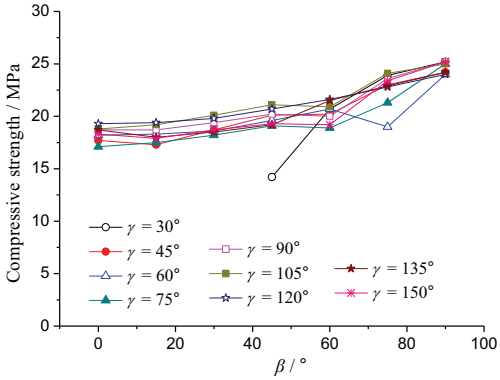

Fig. 6. The numerical results of the compressive strength of the specimens.

When γ stays the same and β varies from 0° to 90°, the uniaxial compressive strength from the numerical simulation also increases gradually. The trend of the changes on the uniaxial compressive strength with the β value obtained from numerical simulations is comparable to the trend obtained from the experimental results.

5. NUMERICAL SIMULATION OF JOINTED ROCK MASS WITH TWO PARALLEL EQUAL-LENGTH JOINT FRACTURES

5. 1 NUMERICAL MODEL

The values of b and $2a$ in Fig. 1 are changed to analyze the effects of these two parameters on the numerical simulation results. When $\beta = 45°$ and $\gamma = 45°$, the numerical simulation models for the various values of b and $2a$ can be seen in Fig. 7.

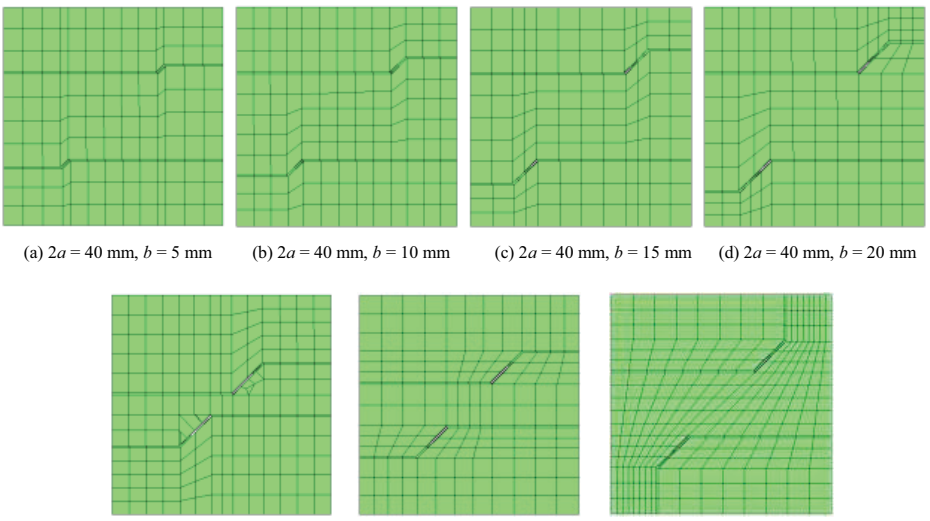

(a) $2a = 40$ mm, $b = 5$ mm (b) $2a = 40$ mm, $b = 10$ mm (c) $2a = 40$ mm, $b = 15$ mm (d) $2a = 40$ mm, $b = 20$ mm

(e) $2a = 10$ mm, $b = 20$ mm (f) $2a = 20$ mm, $b = 20$ mm (g) $2a = 30$ mm, $b = 20$ mm

Fig. 7. Numerical model for specimens with $\beta = 45°$, $\gamma = 45°$, and varied b and $2a$.

5.2 ANALYSIS OF NUMERICAL RESULTS

When $\beta = 0, 45°, 90°$ and $2a = 40$ mm, the effects of b on the strength of the jointed rock specimens are shown in Fig. 8.

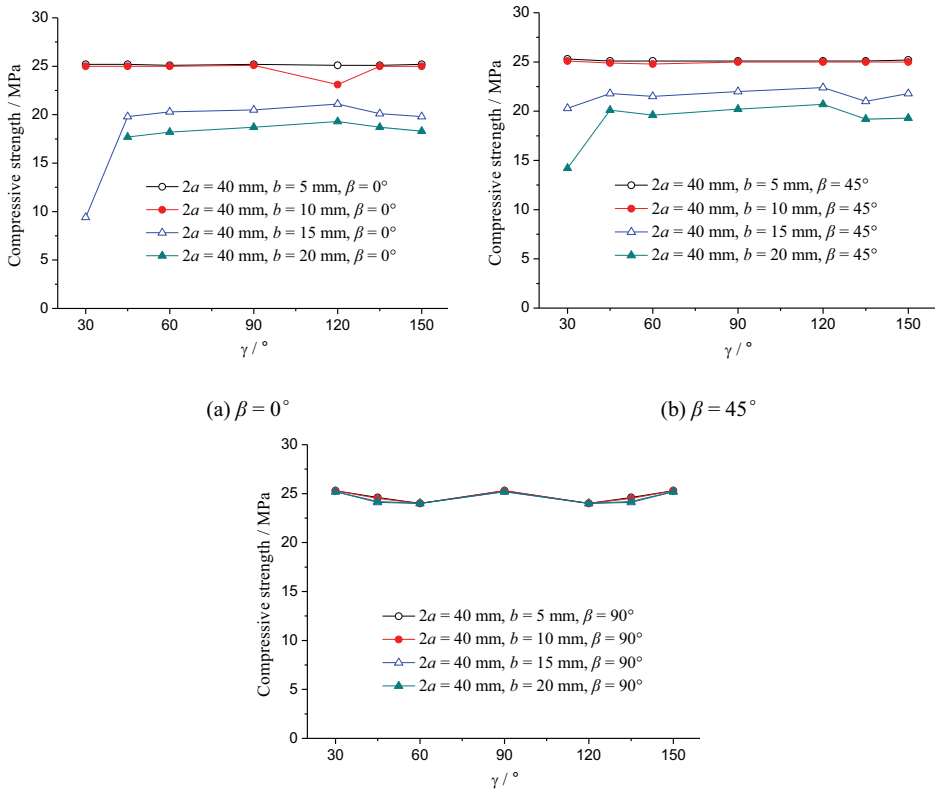

(a) $\beta = 0^\circ$ (b) $\beta = 45^\circ$

(c) $\beta = 90^\circ$

Fig. 8. The effects of b on the strength of the jointed rock specimens when $\beta = 0, 45^\circ, 90^\circ$ and $2a = 40$ mm.

For $\beta = 0°$, $\gamma = 45°$, $2a = 40$ mm, and $\beta = 45°$, $\gamma = 45°$, $2a = 40$ mm, the compressive strength of the jointed rock mass specimen gradually decreases as b increases from 5 mm to 20 mm. For $\beta = 90°$, $\gamma = 45°$ and $2a = 40$ mm, the uniaxial compressive strength of the specimen does not change much when b increases from 5 mm to 20 mm.

When $\beta = 45°$, $\gamma = 45°$, and $b = 20$ mm, the effects of $2a$ on the strength of the jointed rock specimens are shown in Fig. 9.

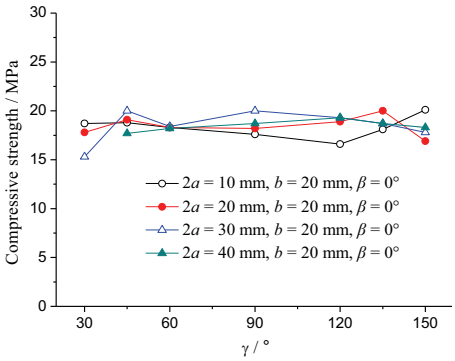

(a) $\beta = 0^\circ$

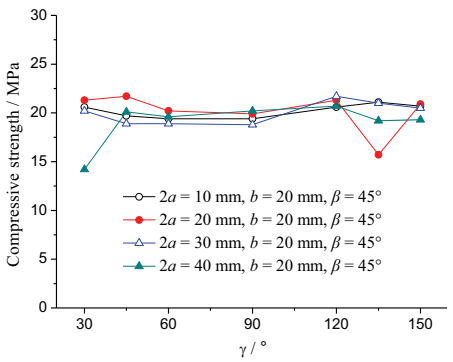

(b) $\beta = 45^\circ$

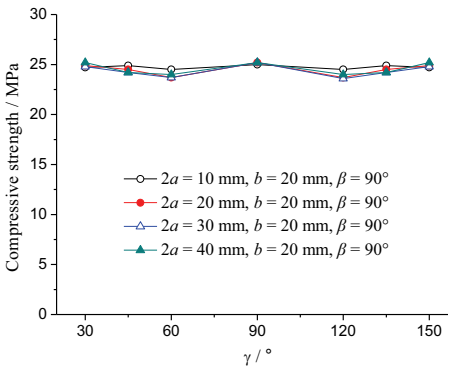

(c) $\beta = 90^\circ$

Fig.9. The effects of $2a$ on the strength of the jointed rock specimens when $\beta = 0, 45^\circ, 90^\circ$ and $b = 20$ mm.

For $\beta = 0°$, $\gamma = 45°$, $b = 20$ mm, and $\beta = 45°$, $\gamma = 45°$, $b = 20$ mm, the change of the compressive strength of the jointed rock mass specimen is not significant and does not show a clear trend when $2a$ increases from 10 mm to 40 mm. For $\beta = 90°$, $\gamma = 45°$, and $b = 20$ mm, the uniaxial compressive strength of the specimen is almost unchanged when $2a$ increases from 10 mm to 40 mm.

6. CONCLUSIONS

1. When the length of the joint fracture, the length of the rock bridge, and the inclination angle of the rock bridge remain unchanged, the uniaxial compressive strength of the specimen increases gradually as the inclination of the joint fracture increases from 0°to 90°.

2. When the length of the joint fracture, the length of the rock bridge, and the inclination of the joint fracture remain unchanged, the uniaxial compressive strength of the specimen does not show a clear trend when the inclination of the rock bridge increases from 30° to 150°.

3. When there is an angle between the joint fracture and the vertical loading direction, if the dip angle of the joint fracture, the inclined angle of the rock bridge, and the length of the rock bridge all remain unchanged, the uniaxial compressive strength of the modeled specimen gradually decreases with an increase in the length of the joint fracture; when the joint fracture coincides with the vertical loading direction, if the dip angle of the joint fracture, the inclined angle of the rock bridge, and the length of the rock bridge all remain unchanged, there is no significant change of the uniaxial compressive strength of the specimen with an increase in the length of the joint fracture.

7. ACKNOWLEDGMENTS

This work was supported by the Open Research Fund of Key Laboratory of Geotechnical and Underground Engineering of Ministry of Education (Grant No. KLE-TJGE-B1505), and the National Natural Science Foundation of China (Grant No. 41541021).

REFERENCES

1. D. Huang, D.M. Gu, C. Yang, R.Q. Huang, G.Y. Fu, “Investigation on mechanical behaviors of sandstone with two preexisting flaws under triaxial compression”, Rock Mech Rock Eng 49: 375-399, 2016.
2. H.Q. Li, L.N.Y.Wong, “Numerical study on coalescence of pre-existing flaw pairs in rock-like material”, Rock Mech Rock Eng, 47: 2087-2105, 2014.
3. J. Zhang, X.P. Zhou, J.Y. Zhu, C. Xian, Y.T. Wang, “Quasi-static fracturing in double-flawed specimens under uniaxial loading the role of strain rate”, Int J Fract, published online, 2018.
4. X.P. Zhang, L.N.Y. Wong, “Crack initiation propagation and coalescence in rock-like material containing two flaws a numerical study based on bonded-particle model approach”, Rock Mech Rock Eng, 47: 1001-1021, 2013.
5. Y.L. Zhao, L.Y. Zhang, W.J. Wang , C.Z. Pu, W. Wan, J.Z. Tang, “Cracking and stress–strain behavior of rock-like material containing two flaws under uniaxial compression”, Rock Mech Rock Eng, 49: 2665-2687, 2016.
6. S.Q. Yang, “Crack coalescence behavior of brittle sandstone samples containing two coplanar fissures in the process of deformation failure”, Engineering Fracture Mechanics, 78: 3059-3081, 2011.
7. S.Q. Yang, W.L.Tian, Y.H. Huang, P.G. Ranjith, Y. Ju, “An experimental and numerical study on cracking behavior of brittle sandstone containing two non-coplanar fissures under uniaxial compression”, Rock Mech Rock Eng, 49, 1497-1515, 2016.

LIST OF FIGURES AND TABLES:

Received 29.09.2018

Revised 30.06.2019